Photochemistry

International Edition: DOI: 10.1002/anie.201809919
German Edition: DOI: 10.1002/ange.201809919

Photoredox/Nickel-Catalyzed Single-Electron Tsuji–Trost Reaction: Development and Mechanistic Insights

Jennifer K. Matsui, Álvaro Gutiérrez-Bonet, Madeline Rotella, Rauful Alam, Osvaldo Gutierrez, and Gary A. Molander**

Abstract: *A regioselective, nickel-catalyzed photoredox allylation of secondary, benzyl, and α-alkoxy radical precursors is disclosed. Through this manifold, a variety of linear allylic alcohols and allylated monosaccharides are accessible in high yields under mild reaction conditions. Quantum mechanical calculations [DFT and DLPNO-CCSD(T)] support the mechanistic hypothesis of a Ni^0 to Ni^{II} oxidative addition pathway followed by radical addition and inner-sphere allylation.*

Over the course of the past 30 years, the Tsuji–Trost allylation has been a workhorse reaction within the field of synthetic organic chemistry.[1] A particularly striking advantage of the Tsuji–Trost reaction is the ability to forge $C(sp^3)$–$C(sp^3)$ bonds under mild reaction conditions, typically using palladium as the transition metal in conjunction with an appropriate phosphine ligand.[2] Although the breadth of electrophilic allyl partners has been quite thoroughly explored, nucleophilic partners have primarily been limited to two-electron carbon- or nitrogen-centered moieties.[3] Specifically, for C–C bond formation, soft nucleophiles (e.g., malonates) are frequently employed, wherein addition occurs by an outer-sphere mechanism.[1]

The choice of nucleophile in these transformations is primarily limited by pK_a constraints, because anions derived from pronucleophiles with pK_a values greater than 25 are not appropriately tuned to react with the incipient π-allyl transition-metal intermediate.[4] Recent reports by Walsh and co-workers have reported the utility of diarylmethane nucleophiles (pK_a up to 32) in palladium-catalyzed allylic substitution reactions, broadening the nucleophile window of Tsuji–Trost reactions.[5] Alternatively, Zn-,[6] Sn-,[7] B-,[8] Mg-,[9] Si-,[10] and Li-based[11] enolates have been used successfully as nucleophilic partners in related transformations.[2b,12] However, a major limitation of enolate-based methods is the prerequisite for highly basic conditions. To overcome these limitations, pioneering work by the group of Tunge shifted efforts toward radical-based intramolecular allylations by a palladium/photoredox cross-coupling, facilitating the decarboxylative allylation of α-amino carboxylic acids. Unfortunately, when Tunge and co-workers moved to intermolecular allylation chemistry, only unsubstituted allyl groups were successfully coupled with alkyl carboxylic acid partners.[13]

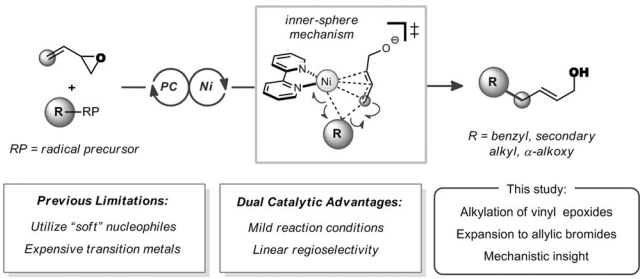

Scheme 1. Exploring radical-based Tsuji–Trost reactivity under photoredox conditions.

Given the excellent precedent for merging photoredox and nickel catalysis in alkylation reactions established by our group and others,[14] we sought to expand this paradigm to radical-based Tsuji–Trost reactions (Scheme 1). In particular, numerous radical precursors (e.g., alkyltrifluoroborates, carboxylates, alkylsilicates, and 1,4-dihydropyridines) derived from diverse commodity chemicals have been developed.[15] Although such reagents have been extensively utilized in conjunction with photoredox/nickel dual cross-coupling with aryl[16] and alkenyl[17] electrophiles, we have also begun to expand the scope of electrophilic partners for such transformations (e.g., using isocyanate,[18] acyl chloride,[19] carboxylic acid,[20] and acyl imide electrophiles[21]). In a continuation of that effort, the cost-effective nature of nickel-based catalysts and the slow β-hydride elimination of alkylnickel species, relative to that of palladium, was considered for investigating how this approach could be applied to the Tsuji–Trost reaction.[22]

Vinyl epoxides have been employed previously in palladium-catalyzed allylations,[23] but to the best of our knowledge, reports using a nickel-based catalyst—a nonprecious, inexpensive catalyst—are scarce,[24] with only a few examples being reported involving cycloaddition reactions. At the outset of substrate exploration, a variety of benzyltrifluoroborates were selected. Early results demonstrated a diversity of electron-withdrawing and electron-donating groups were accommodated (Table 1). Additionally, modestly sterically

[*] Dr. J. K. Matsui, Dr. Á. Gutiérrez-Bonet, Dr. R. Alam, Prof. G. A. Molander
Department of Chemistry
University of Pennsylvania
Roy and Diana Vagelos Laboratories
Philadelphia, PA 19104-6323 (USA)
E-mail: gmolandr@sas.upenn.edu
M. Rotella, Prof. O. Gutierrez
Department of Chemistry and Biochemistry
University of Maryland
College Park, MD 20742 (USA)
E-mail: ogs@umd.edu
Supporting information and the ORCID identification number(s) for the author(s) of this article can be found under: https://doi.org/10.1002/anie.201809919.

Table 1: Radical scope

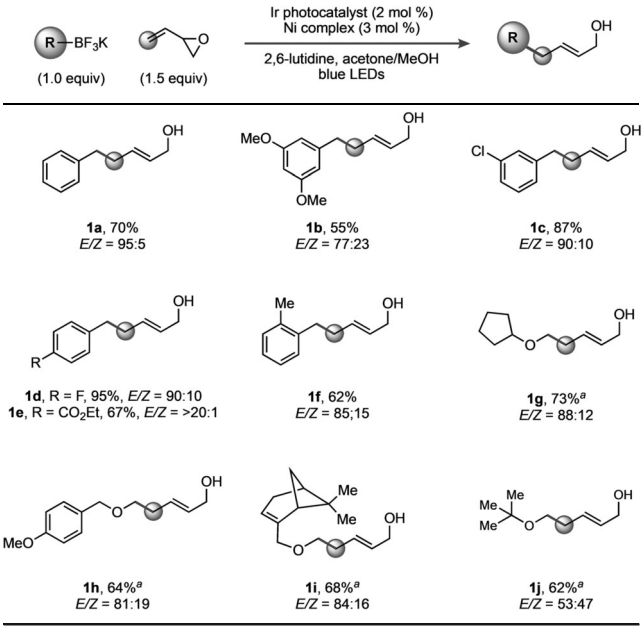

Reactions were conducted on 0.50 mmol scale. Standard reaction conditions employed butadiene monoxide (1.0 equiv), alkyltrifluoroborate (1.5 equiv), $Ir[dFCF_3ppy]_2(bpy)PF_6$ (2 mol%), $[Ni(dtbbpy)(H_2O)_4]Cl_2$ (3 mol%), and 2,6-lutidine (3.5 equiv) in acetone/MeOH (9:1). See Supporting Information for more details. [a] For α-alkoxyalkyltrifluoroborates, a solvent mixture of acetonitrile/*tert*-butanol (10:1) was used.

Table 2: Diversifying the vinyl epoxide backbone

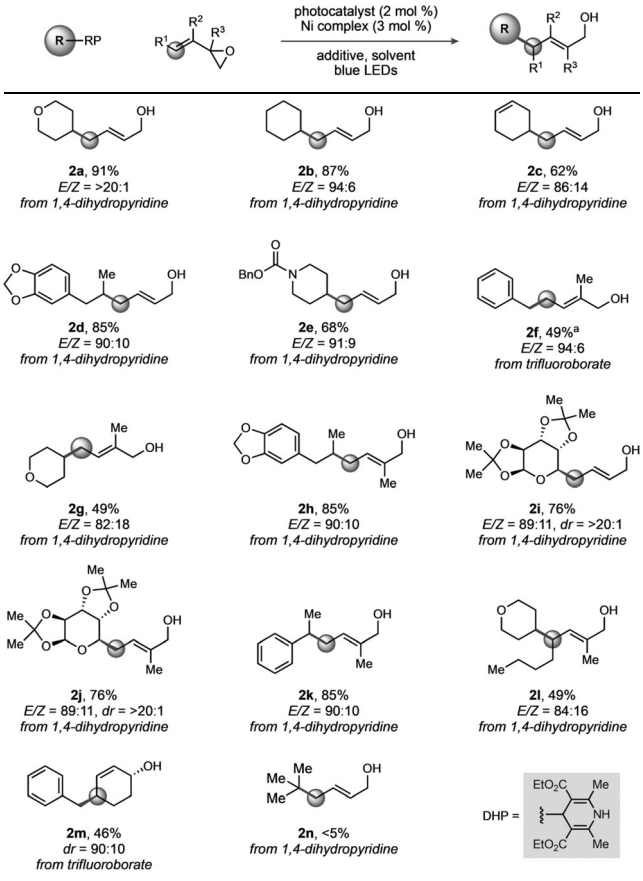

Reactions were conducted on 0.50 mmol scale. Standard reaction conditions employed butadiene monoxide (1.0 equiv), 1,4-dihydropyridine (1.5 equiv), 4CzIPN (2 mol%), and $[Ni(dtbbpy)(H_2O)_4]Cl_2$ (3 mol%) in acetone. For trifluoroborates, standard reaction conditions employed butadiene monoxide (1.0 equiv), alkyltrifluoroborate (1.5 equiv), $Ir[dFCF_3ppy]_2(bpy)PF_6$ (2 mol%), $[Ni(dtbbpy)(H_2O)_4]Cl_2$ (3 mol%), and 2,6-lutidine (3.5 equiv) in acetone/MeOH (9:1). For α-alkoxyalkyltrifluoroborates, a solvent mixture of acetonitrile/*tert*-butanol (10:1) was used. See Supporting Information for more details.

hindered substrates could also be used. For example, *ortho* substitution afforded 62% of desired product **1f**. As the radical-precursor search was expanded, α-alkoxytrifluoroborates were next targeted. Generally, *E*/*Z* selectivity was high, although the ratio was severely diminished to 53:47 when *tert*-butyl ether moieties were explored (**1j**).

Moving forward, the breadth of carbon-centered radicals was expanded by targeting unstabilized secondary alkyl radical precursors. Under the standard and modified reaction conditions, secondary alkyltrifluoroborates formed complex mixtures (e.g., homocoupling, aldehydic side products).[25] Therefore, DHPs (1,4-dihydropyridines) were investigated as alternative radical precursors[26,27] with 4CzIPN (2,4,5,6-tetra(9*H*-carbazol-9-yl)isophthalonitrile) as an organophotocatalyst (Table 2). During the exploration of various DHPs, heterocyclic (**2a** and **2e**) and alkenyl moieties (**2c**) were successfully incorporated within the coupling partners under the optimized reaction conditions. A desire to integrate greater functional density within the radical precursor led to the exploration of monosaccharide moieties that were recently highlighted in publications from our group.[28] Pleasingly, pyranose DHP afforded the allylated product **2i** in high *E*/*Z* ratios and diastereoselectivity.

Subsequently, substitution on the vinyl epoxide moiety was probed, starting with methyl substitution on the requisite epoxide (**2f–h**; Table 2). Notably, the stereochemical outcome of the photoredox/nickel dual catalyzed alkylation is complementary to that of the palladium-catalyzed transformations. The latter provided net retention by double inversion,[26] whereas in the present case 1,2-epoxy-3,4-cyclohexene afforded primarily the *trans* isomer (**2m**), suggesting the nickel coordinates the alkene and adds to the opposite face of the epoxide, but then the resulting nickel complex engages the radical and undergoes reductive elimination by a stereoretentive, inner-sphere mechanism. This hypothesis was further supported by both DFT and DLPNO-CCSD(T) quantum mechanical calculations.

Finally, although the allylic alcohol products themselves are versatile moieties,[29] we aimed to make the protocol more general by exploring electrophiles as π-allylnickel precursors (Table 3). First, various leaving groups were surveyed (i.e., bromide, chloride, and carbonate), with allyl bromide affording the highest yield of product under the initial reaction conditions.

Motivated by the advantageous biological properties demonstrated by molecules containing alkyl-substituted carbohydrate substructures,[30] DHP monosaccharides were successfully allylated under the dual catalytic conditions with modest to high diastereoselectivities (Table 4). Pyranose and

Table 3: Expanding the scope with respect to the allylic substrate.

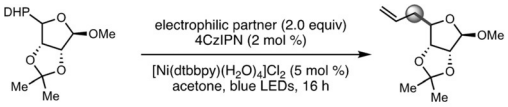

entry	electrophilic partner	% yield
1		78
2		<20
3	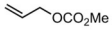	60

Yields are those of the isolated products.

Table 4: Allylation of monosaccharide DHPs

allyl bromide	*1,4-dihydropyridine*	*product*	*% yield (dr)*
	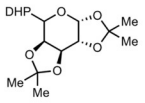	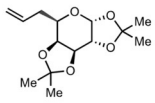	**4a**, 70 (>20:1)
	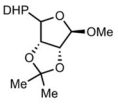	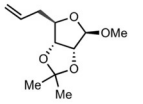	**4b**, 97 (>20:1)
	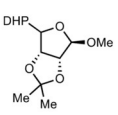	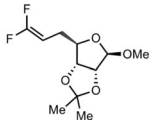	**4c**, 94 (>20:1)

All reactions were performed using 0.75 mmol of allyl bromide, 0.25 mmol of 1,4-dihydropyridine, 4CzIPN (2 mol%), and [Ni(dtbbpy)-$(H_2O)_4$]Cl_2 (3 mol%) in acetone with blue LED irradiation for 24 h. See Supporting Information for more details.

furanose backbones with benzyl, methoxy, and dioxolane protecting groups were conserved. Further studies on substituent effects were conducted using difluoroallyl bromide. Under the established reaction conditions, **4c** was isolated as a single regioisomer. Presumably, oxidative addition to allyl bromide followed by bromide expulsion generates the key π-allylnickel complex which, by an inner-sphere mechanism, intercepts the α-alkoxy radical to undergo diastereoselective reductive elimination, forming the allylated products.

Intrigued by the stereoselectivity of these processes and questions regarding the order of reaction events, quantum mechanical calculations were undertaken to gain insight into the underlying mechanism of this transformation.[31] As shown in Figure 1 (squares), complexation of Ni^0 to vinyl epoxide (**A″**) is energetically favored over that of complexation to benzyl radical (**A′**; presumably formed from the photocatalytic cycle, see the Supporting Information for energetics) by 8.9 kcal mol^{-1}. Subsequently, this vinyl epoxide/Ni^0 (**A″**) complex can quickly undergo an S_N2-like ring-opening (via **A″-TS**; barrier is only 3.1 kcal mol^{-1} from **A″**) to form the π-allylnickel(II) intermediate **B″**. As anticipated by previous calculations,[32] **B″** can quickly engage the benzyl radical, generated by single-electron transfer (SET) oxidation of $BnBF_3K$ by the photocatalyst (see the Supporting Information for energetics), to form the Ni^{III} intermediate **C** (via **B″-C-TS**). Overall, radical addition is facile (the barrier is ca. 1–3 kcal mol^{-1}, dependent on the method). Finally, inner-sphere $C(sp^2)$–$C(sp^3)$ bond formation via **C-TS$_L$** (the barrier is 8.9 kcal mol^{-1} from **C**) leads to formation of the linear product (**P$_L$**), 50.3 kcal mol^{-1} downhill in energy.

A series of reductive elimination transition states leading to formation of branched products (e.g., **C-TS$_B$**) were also located, but these were much higher in energy (> 5 kcal mol^{-1}) than **C-TS$_L$**, presumably because of unfavorable electronic repulsion and steric interactions between the charged oxygen and the benzyl group (Figure 1). Moreover, $C(sp^2)$–$C(sp^3)$ bond formation by an outer-sphere pathway (squares and triangles) was also found higher in energy. Formation of **C** from a Ni^0-Ni^I-Ni^{III} pathway (Figure 1, circle) is also overall higher in energy than the Ni^0-Ni^{II}-Ni^{III} pathway (squares). Albeit low, the barrier for radical addition (**A-TS**) from Ni^0 is still 7.3 kcal mol^{-1} higher in energy than oxidative addition to vinyl epoxide (via **A″-TS**). However, it is likely

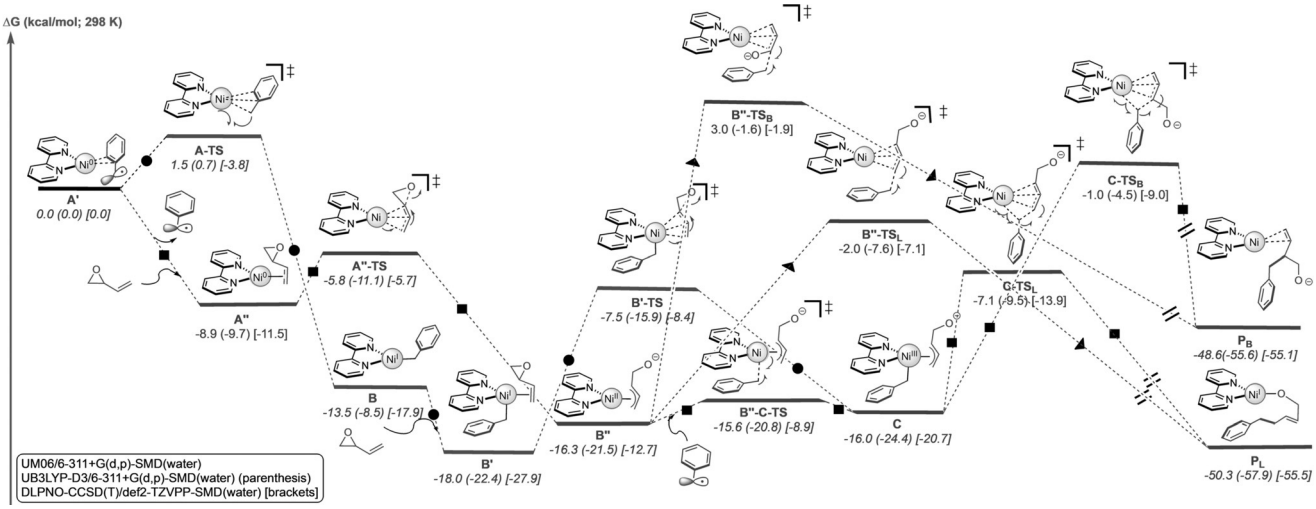

Figure 1. Competing Ni^0/Ni^I/Ni^{III} (circles), Ni^0/Ni^{II}/Ni^{III} (squares), Ni^0/Ni^{II} (squares and triangles), pathways leading to $C(sp^3)$–$C(sp^3)$ bond formation.

that formation of **C** is highly dependent on the local concentration of the benzyl radical and vinyl epoxide. Overall, DFT and DLPNO-CCSD(T) calculations support a Ni^0-Ni^{II}-Ni^{III} reaction pathway and an inner-sphere reductive elimination as the product-determining step, leading to formation of the linear product as the major product.[33] This model is in accord with the stereochemical results observed with cyclohexadiene monoxide (**2m**; Table 1,). Further, although computational studies favored the linear product, the branched pathway is only 5 kcal mol^{-1} higher in energy, suggesting branched products may be observed in some cases (likely dependent on the nature of the substrate, ligand, etc.). To test this hypothesis, we subjected sterically hindered aryl-substituted vinyl epoxides to the standard reaction conditions and indeed found a mixture of linear and branched products, albeit in low yields (Scheme 2).

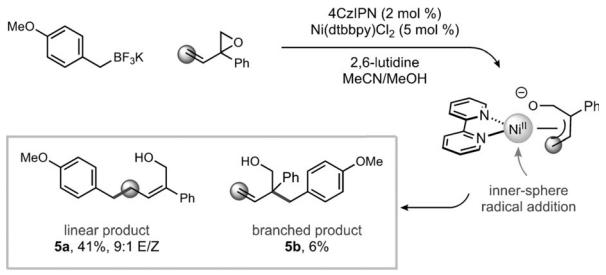

Scheme 2. Observation of mixtures of linear and branched products.

In summary, a dual catalytic allylation reaction is reported and demonstrates complementarity to traditional Tsuji–Trost reactions. In juxtaposition with classical reactivity in the palladium-catalyzed transformations (stabilized anionic carbon nucleophiles), carbon-centered radicals were employed, enabling the allylation of secondary, benzyl, and α-alkoxy radical precursors. Additionally, net inversion of stereochemistry is observed in the photoredox/nickel dual catalyzed systems, as opposed to the net retention by double inversion observed in the traditional palladium-catalyzed processes.

To gain insight into the mechanistic pathway, studies incorporating quantum mechanical calculations [using dispersion corrected (U)DFT and DLPNO-CCSD(T) methods] were conducted to determine the energetic favorability of the oxidative addition step. Here, a Ni^0 to Ni^{II} oxidative addition step was calculated to occur before radical addition to the nickel center. This proposal is a deviation from previous mechanistic studies of photoredox/nickel dual cross-coupling pathways where Ni^0 to Ni^I has been involved in the putative pathway.[32] Given the mild reaction conditions and availability of numerous radical precursors, the disclosed method provides a useful complement to the traditional, palladium-catalyzed Tsuji–Trost reaction.

Acknowledgements

We are grateful for the financial support provided by NIGMS (R01 GM 113878 to G.M.) and NSF (CAREER, 1751568 to O.G.). J.K.M. is supported by the Bristol-Myers Squibb Graduate Fellowship for Synthetic Organic Chemistry. O.G. is grateful to the University of Maryland College Park for start-up funds and computational resources from UMD Deepthought2 and MARCC/BlueCrab HPC clusters and XSEDE (CHE160082 and CHE160053). We thank Dr. Charles W. Ross, III (University of Pennsylvania) for assistance in obtaining HRMS data. Additionally, Dr. Jun Gu (University of Pennsylvania) and Matt Bunner (University of Pennsylvania) assisted in the acquisition and analysis of NMR data. The alkyltrifluoroborates and the iridium (for photocatalyst synthesis) were generously donated by Frontier and Johnson-Matthey, respectively.

Conflict of interest

The authors declare no conflict of interest.

Keywords: allylic compounds · nickel · photochemistry · reaction mechanisms · synthetic methods

How to cite: *Angew. Chem. Int. Ed.* **2018**, *57*, 15847–15851
Angew. Chem. **2018**, *130*, 16073–16077

[1] B. M. Trost, *Acc. Chem. Res.* **1980**, *13*, 385–393.
[2] a) J. Tsuji, *Organic Synthesis with Palladium Compounds*, Springer, New York, **1980**; b) B. M. Trost, D. L. Van Vranken, *Chem. Rev.* **1996**, *96*, 395–422.
[3] a) G. Consiglio, R. M. Waymouth, *Chem. Rev.* **1989**, *89*, 257–276; b) A. Heumann, M. Reglier, *Tetrahedron* **1995**, *51*, 975–1015.
[4] B. M. Trost, M. R. Machacek, A. Aponick, *Acc. Chem. Res.* **2006**, *39*, 747.
[5] S.-C. Sha, J. Zhang, P. J. Carroll, P. J. Walsh, *J. Am. Chem. Soc.* **2013**, *135*, 17602–17609.
[6] S. Son, G. C. Fu, *J. Am. Chem. Soc.* **2008**, *130*, 2756–2757.
[7] a) B. M. Trost, C. R. Self, *J. Org. Chem.* **1984**, *49*, 468–473; b) B. M. Trost, E. Keinan, *Tetrahedron Lett.* **1980**, *21*, 2591–2594.
[8] E. Negishi, H. Matsushita, S. Chatterjee, R. A. John, *J. Org. Chem.* **1982**, *47*, 3188–3190.
[9] M. Braun, T. Meier, *Angew. Chem. Int. Ed.* **2006**, *45*, 6952–6955; *Angew. Chem.* **2006**, *118*, 7106–7109.
[10] T. Graening, J. F. Hartwig, *J. Am. Chem. Soc.* **2005**, *127*, 17192–17193.
[11] B. M. Trost, G. M. Schroeder, *J. Am. Chem. Soc.* **1999**, *121*, 6759–6760.
[12] M. Braun, *Helv. Chim. Acta* **2015**, *98*, 1–31.
[13] S. B. Lang, K. M. O'Nele, J. A. Tunge, *J. Am. Chem. Soc.* **2014**, *136*, 13606–13609.
[14] a) J. C. Tellis, D. N. Primer, G. A. Molander, *Science* **2014**, *345*, 433–436; b) Z. Zuo, D. T. Ahneman, L. Chu, J. A. Terett, A. G. Doyle, D. W. C. MacMillan, *Science* **2014**, *345*, 437–440.
[15] a) V. Corcé, L.-M. Chamoreau, E. Derat, J.-P. Goddard, C. Ollivier, L. Fensterbank, *Angew. Chem. Int. Ed.* **2015**, *54*, 11414–11418; *Angew. Chem.* **2015**, *127*, 11576–11580; b) M. Jouffroy, D. N. Primer, G. A. Molander, *J. Am. Chem. Soc.* **2016**, *138*, 475–478; c) K. Nakajima, S. Nojima, Y. Nishibayashi, *Angew. Chem. Int. Ed.* **2016**, *55*, 14106–14316; *Angew. Chem.* **2016**, *128*, 14312–14316; d) A. Gutiérrez-Bonet, J. C. Tellis, J. K. Matsui, B. A. Vara, G. A. Molander, *ACS Catal.* **2016**, *6*, 8004–8008.
[16] Reviews on photoredox catalysis: a) J. C. Tellis, C. B. Kelly, D. N. Primer, M. Jouffroy, N. R. Patel, G. A. Molander, *Acc. Chem.*

Res. **2016**, *49*, 1429 – 1439; b) J. K. Matsui, S. B. Lang, D. R. Heitz, G. A. Molander, *ACS Catal.* **2017**, *7*, 2563 – 2575; c) C. K. Prier, D. A. Rankic, D. W. C. MacMillan, *Chem. Rev.* **2013**, *113*, 5322 – 5363; d) M. N. Hopkinson, B. Sahoo, J.-L. Li, F. Glorius, *Chem. Eur. J.* **2014**, *20*, 3874 – 3886.

[17] N. R. Patel, C. B. Kelly, M. Jouffroy, G. A. Molander, *Org. Lett.* **2016**, *18*, 764 – 767.

[18] S. Zheng, D. N. Primer, G. A. Molander, *ACS Catal.* **2017**, *7*, 7957 – 7961.

[19] a) J. Amani, E. Sodagar, G. A. Molander, *Org. Lett.* **2016**, *18*, 732 – 735; b) J. Amani, G. A. Molander, *Org. Lett.* **2017**, *82*, 1856 – 1863.

[20] J. Amani, G. A. Molander, *Org. Lett.* **2017**, *19*, 3612 – 3615.

[21] J. Amani, R. Alam, S. Badir, G. A. Molander, *Org. Lett.* **2017**, *19*, 2426 – 2429.

[22] S. Z. Tasker, E. A. Standley, T. F. Jamison, *Nature* **2014**, *509*, 299 – 309.

[23] B. M. Trost, G. A. Molander, *J. Am. Chem. Soc.* **1981**, *103*, 5969 – 5972. For an extensive review article, see: J. He, J. Ling, P. Chiu, *Chem. Rev.* **2014**, *114*, 8037 – 8128.

[24] S. Crotti, F. Bertolini, F. Macchia, M. Pineschi, *Org. Lett.* **2009**, *11*, 3762. During the course of our studies, Gong and co-workers published a method describing a reductive allylation of tertiary alkyl halides using allylic carbonates: H. Chen, X. Jia, Y. Yu, Q. Qian, H. Gong, *Angew. Chem. Int. Ed.* **2017**, *56*, 13103 – 13106; *Angew. Chem.* **2017**, *129*, 13283 – 13286. Their report includes deuterium studies supporting the formation of a π-allylnickel intermediate.

[25] Secondary alkyltrifluoroborates have significantly high reduction potentials at +1.50 V vs. SCE (see D. N. Primer, K. Karakaya, J. C. Tellis, G. A. Molander, *J. Am. Chem. Soc.* **2015**, *137*, 2195 – 2198).

[26] a) N. Tewari, N. Dwivedi, R. Tripathi, *Tetrahedron Lett.* **2004**, *45*, 9011 – 9014; b) H. Adibi, H. A. Samimi, M. Beygzadeh, *Catal. Commun.* **2007**, *8*, 2119 – 2124; c) A. Heydari, S. Khaksar, M. Tajbakhsh, H. R. Bijanzadeh, *J. Fluorine Chem.* **2009**, *130*, 609 – 614; d) D. Zhang, L.-Z. Wu, L. Zhou, X. Han, Q.-Z. Yang, L.-P. Zhang, C.-H. Tung, *J. Am. Chem. Soc.* **2004**, *126*, 3440 – 3441; e) X. Wei, L. Wang, W. Jia, S. Du, L. Wu, Q. Liu, *Chin. J. Chem.* **2014**, *32*, 1245 – 1250; f) S. Fukuzumi, T. Suenobu, M. Patz, T. Hirasaka, S. Itoh, M. Fujitsuka, O. Ito, *J. Am. Chem. Soc.* **1998**, *120*, 8060 – 8068; g) D. Wang, Q. Liu, B. Chen, L. Zhang, C. Tung, L. Wu, *Chin. Sci. Bull.* **2010**, *55*, 2855 – 2858.

[27] a) K. Nakajima, S. Nojima, K. Sakata, Y. Nishibayashi, *ChemCatChem* **2016**, *8*, 1028 – 1032; b) W. Chen, Z. Liu, J. Tian, J. Li, J. Ma, X. Cheng, G. Li, *J. Am. Chem. Soc.* **2016**, *138*, 12312 – 12315; c) L. Buzzetti, A. Prieto, S. R. Roy, P. Melchiorre, *Angew. Chem. Int. Ed.* **2017**, *56*, 15039 – 15043; *Angew. Chem.* **2017**, *129*, 15235 – 15239; d) C. Verrier, N. Alandini, C. Pezzetta, M. Moliterno, L. Buzzetti, H. B. Hepburn, A. Vega-Penaloza, M. Silvi, P. Melchiorre, *ACS Catal.* **2018**, *8*, 1062 – 1066. For a recent review, see: W. Huang, X. Cheng, *Synlett* **2017**, *28*, 148 – 158.

[28] a) S. O. Badir, A. Dumoulin, J. K. Matsui, G. A. Molander, *Angew. Chem. Int. Ed.* **2018**, *57*, 6610 – 6613; *Angew. Chem.* **2018**, *130*, 6720 – 6723; b) A. Dumoulin, J. K. Matsui, A. Gutierrez-Bonet, G. A. Molander, *Angew. Chem. Int. Ed.* **2018**, *57*, 6614 – 6618; *Angew. Chem.* **2018**, *130*, 6724 – 6728.

[29] N. A. Butt, W. Zhang, *Chem. Soc. Rev.* **2015**, *44*, 7929 – 7967.

[30] a) Z. G. Khalil, A. A. Salim, D. Vuong, A. Crombie, E. Lacey, A. Blumental, R. J. Capon, *J. Antibiot.* **2017**, *70*, 1097 – 1103; b) M. Bayliss, M. I. Donaldson, S. A. Nepogodiev, G. Pergolizzi, A. E. Scott, N. J. Harmer, R. A. Field, J. L. Prior, *Carbohydr. Res.* **2017**, *452*, 17 – 24; synthetic efforts: c) S. Zhao, N. P. Mankad, *Angew. Chem. Int. Ed.* **2018**, *57*, 5867 – 5870; *Angew. Chem.* **2018**, *130*, 5969 – 5972; d) A. Szekrenyi, X. Garrabou, T. Parella, J. Joglar, J. Bujons, P. Clapes, *Nat. Chem.* **2015**, *7*, 724 – 729.

[31] For all of the calculations, dispersion-corrected, broken-spin (U)DFT functionals (UM06/6–311 + G(d,p)-SMD(water)//UB3LYP/6-31G(d) and UB3LYP-D3/6–311 + G(d,p)-SMD(water)//UB3LYP/6-31G(d)) were used. Further, the energy profile using dynamic correlation, open-shell domain-based local pair natural orbital coupled-cluster calculations (DLPNO-CCSD(T)/def2-TZVPP-SMD(water)//UB3LYP/6-31G(d)) were compared, which are known to provide accurate energies (within 3 kJ mol^{-1}) with the computational cost comparable to DFT calculations. Overall, all methods provided similar conclusions (see the Supporting Information for further details). For simplicity, only UM06/6–311 + G(d,p)-SMD(water)//UB3LYP/6-31G(d) energies will be discussed in the manuscript.

[32] O. Gutierrez, J. C. Tellis, D. N. Primer, G. A. Molander, M. C. Kozlowski, *J. Am. Chem. Soc.* **2015**, *137*, 4896 – 4899.

[33] We also considered the protonation of **B″** followed by: 1) outer-sphere C(sp^2)–C(sp^3) bond formation and 2) radical addition, with subsequent inner-sphere C(sp^2)–C(sp^3) bond formation. However, the barriers for both protonated inner-sphere and outer-sphere pathways were higher in energy than the anionic pathway (see the Supporting Information).

Manuscript received: August 28, 2018
Revised manuscript received: September 27, 2018
Accepted manuscript online: October 11, 2018
Version of record online: November 7, 2018

